

Adaptive Multi-Objective Optimization Of PV-Diesel Hybrid Systems For Climate Resilience In Semi-Arid Regions

ADIMANANA Ruben Mahaliny^{1, 2, *}, LALASON Todisoa Antonio¹, NOMENJANAHARY Elie Solosene³, FANAMPISOA Béatrice Milasoa³, RISITE Heriarivelo², RANDRIANANTENAINA Jean Eugène^{1,2}

¹ Doctoral School of Geosciences, Physics, Environmental Chemistry, and Host-Pathogen Systems
² Faculty of Science and Technology, University of Toliara

³ Institute of Higher Education of Toliara

Corresponding Author: ADIMANANA Ruben Mahaliny, +261 34 15 923 37 / +261 32 13 951 65 / E-mail: mahalinyadimanana@gmail.com



Abstract – The electrification of semi-arid regions confronts unprecedented reliability challenges stemming from extreme climate variability challenges that climate change continues to intensify at an accelerating pace. Conventional optimization methods for PV-diesel hybrid systems often fail to account for these deep uncertainties, leading to designs that are either unreliable or economically unviable. This paper introduces a novel Adaptive Multi-Objective Genetic Algorithm with an Evolving Fitness Function (AMOGA-EFF) to optimize system design for long-term resilience. The framework is uniquely built on a comprehensive uncertainty analysis, integrating high-resolution stochastic modeling from 20-year historical weather data with an ensemble of CMIP6 climate projections (SSP2-4.5 and SSP5-8.5). To quantify performance under these stresses, we introduce two new metrics: the Climate Robustness Index (CRI) and the Economic Vulnerability Factor (EVF).

The AMOGA-EFF approach was rigorously tested through extensive simulations for three distinct sites: Ouagadougou (Burkina Faso), Jodhpur (India), and Petrolina (Brazil); where it consistently demonstrated superior performance. It yields a 35-42% improvement in system resilience with only a 6-11% increase in the levelized cost of energy (LCOE) compared to the standard NSGA-II algorithm. Under the high-emission SSP5-8.5 scenario, optimized systems maintain 89% availability during extreme weather events, in stark contrast to the 61% achieved by conventional deterministic designs. Furthermore, the resulting configurations achieve a 13.3% reduction in total life-cycle cost, primarily through a 22.1% decrease in fuel consumption. This work provides a robust methodological blueprint for designing resilient and cost-effective energy infrastructures in climate-vulnerable regions worldwide.

Keywords: Multi-objective optimization; PV-diesel hybrid; Climate change; CMIP6; Semi-arid regions; Adaptive genetic algorithm; Stochastic optimization

1. INTRODUCTION

The electrification of semi-arid regions, home to nearly two billion people, faces the challenge of high solar variability (CV > 30%), a factor amplified by climate change. Current PV-diesel optimization methodologies fail to simultaneously integrate historical uncertainty and CMIP6 projections, resulting in undersized systems. This paper presents an adaptive genetic algorithm that incorporates 10,000 stochastic scenarios and climate projections, along with two new resilience metrics (CRI, EVF).

2. LITERATURE REVIEW

Current optimization approaches for hybrid systems are constrained by three major research gaps. First, conventional multiobjective algorithms such as NSGA-II, MOPSO, and GA-PSO achieve localized improvements (18-22%) but rely on deterministic

Vol. 54 No. 1 December 2025 ISSN: 2509-0119 110



climate data; consequently, they ignore real-world climate variability. Second, existing stochastic approaches are either partial (e.g., considering only load uncertainty), computationally prohibitive or statistically insufficient. Third, the integration of climate change remains rudimentary, typically neglecting the non-linear dynamics captured in CMIP6 projections.

To date, no single study has simultaneously integrated high-resolution historical variability, statistically downscaled CMIP6 projections, and multi-site operational validation. This constitutes a critical methodological gap for achieving resilient electrification.

3. METHODOLOGIES

3.1 Study Sites and Data

To ensure the robustness and generalizability of our findings, three representative sites were selected based on their Köppen-Geiger classification (BSh - hot semi-arid climate), geographical distribution, and data availability:

Site 1: Ouagadougou, Burkina Faso (12.35°N, 1.53°W)

- Population served: 500 households
- Load profile: 680 kWh/day (peak: 85 kW)
- Existing system: 150 kWp PV + 120 kW diesel (operational since 2018)

Site 2 : Jodhpur, India (26.30°N, 73.02°E)

- Population served: 350 households + irrigation pumps
- Load profile: 520 kWh/day (peak: 75 kW)
- Existing system: 100 kWp PV + 100 kW diesel (operational since 2019)

Site 3: Petrolina, Brazil (9.39°S, 40.50°W)

- Population served: 400 households + agro-processing unit
- Load profile: 750 kWh/day (peak: 95 kW)
- Existing system: 180 kWp PV + 150 kW diesel (operational since 2017)

Historical climate data for the 2003-2022 period were obtained from SYNOP/METAR stations, NASA POWER, and the ERA5 reanalysis dataset.

Vol. 54 No. 1 December 2025 ISSN: 2509-0119 111

Table 1: Climate characteristic	s of sti	ıdv sites	(2003-2022 average)

D	Ouagadougou		Jodhpur		Petrolina	
Parameter	Mean	CV (%)	Mean	CV (%)	Mean	CV (%)
Daily GHI (kWh/m²)	5.92	28.3	5.64	31.2	5.78	25.7
Temperature (°C)	28.7	12.4	26.3	18.6	27.1	10.2
Dust events/year	42	35.1	58	41.3	18	28.6
Extreme event frequency*	0.12	-	0.15	-	0.09	-

^{*}Defined as consecutive days with GHI < 3rd percentile

3.2 System Modeling and Energy Management

PV Model with Dust Soiling Effects:

SN:2509-0119 https://ijpsat.org/

$$P_{PV}(t) = N_{PV} \cdot P_{STC} \cdot \frac{G_T(t)}{G_{STC}} \cdot [1 + \alpha_P(T_C(t) - T_{STC})] \cdot \eta_{dust}(t) \cdot \eta_{deg}(t)$$
 (1)

Where $\eta_{dust}(t) = 1 - \beta_d \cdot t_d \, \text{si} \, t_d < t_{clean}$, with a site-specific dust coefficient β_d ranging from 0,003 - 0,008 per day. Diesel Generator Model with Environmental Corrections:

$$F(t) = (a_0 + a_1 \cdot P_{gen} + a_2 \cdot P_{gen}^2 + a_3 \cdot P_{gen}^3) \cdot K_{alt} \cdot K_{temp}(T) \cdot K_{age}$$
 (2)

Battery Model with Temperature-Dependent Aging:

$$\frac{dSoH}{dt} = -k_{cal} \cdot exp\left(\frac{-E_a}{R \cdot T_{bat}}\right) - k_{cyc} \cdot \sqrt{DoD} \cdot |I_{bat}|$$
 (3)

Energy management strategy:

Our energy management strategy employs a hierarchical rule-based framework that prioritizes photovoltaic self-consumption while treating diesel generation as the option of last resort. The dispatch priorities are as follows: meet the load with PV; manage excess generation; manage energy deficit; diesel generator as last resort.

3.3 Climate Scenario Generation with CMIP6

We employed a hybrid approach combining Markov Chain Monte Carlo (MCMC) with Copula functions to preserve both temporal autocorrelation and inter-variable dependencies in the climate data. The process involves several rigorous steps: historical data analysis; dependency modeling; weather regime identification; stochastic scenario generation.

We utilized 5 global climate models from CMIP6: CNRM-CM6-1, GFDL-ESM4, IPSL-CM6A-LR, MRI-ESM2-0, UKESM1-0-LL provide SSP2-4.5 and SSP5-8.5 projections.

3.4 Multi-Objective Optimization Problem Formulation

Decision Variables:
$$x = [N_{PV}, C_{bat}, P_{diesel}, N_{clean}]^T$$
 (4)

Objective Functions:

Expected Levelized Cost of Energy (LCOE):

$$F_{1}(x) = \mathbb{E}_{s \in S} \left[\frac{\sum_{t=0}^{T} \frac{C_{cap,t} + C_{0\&M,t}(s) + C_{fuel,t}(s) + C_{rep,t}}{(1+r)^{t}}}{\sum_{t=0}^{T} \frac{E_{served,t}(s)}{(1+r)^{t}}} \right]$$
 (5)

Expected Loss of Power Supply Probability (LPSP):

$$F_2(x) = \mathbb{E}_{s \in S} \left[\frac{\sum_{h=1}^{8760} 1[P_{supply}(h,s) < P_{load}(h)]}{8760} \right]$$
 (6)

Climate Robustness Index (CRI), our proposed metric:

$$F_3(x) = \frac{VaR_{0,95}(LPSP) - \mathbb{E}[LPSP]}{\mathbb{E}[LPSP]} \times \frac{max_{s \in S_{extreme}}[Duration_{failure}]}{168}$$
(7)

ISSN: 2509-0119

Economic Vulnerability Factor (EVF), our proposed metric:

$$F_4(x) = \frac{\sigma_{LCOE}}{\mu_{LCOE}} \times \left(1 + \frac{LCOE_{CC,2050} - LCOE_{hist}}{LCOE_{hist}}\right)$$
(8)

3.5 Algorithmic AMOGA-EFF:

The proposed AMOGA-EFF algorithm extends the NSGA-II framework with four key innovations. Its operational logic is structured as follows:

- Initialization
- Adaptive Control
- Progressive Fitness Evolution

https://ijpsat.org/

• Evolutionary Operations and Selection

4. RESULTS

This section presents the multifaceted outcomes of our study. The analysis is structured to first quantify the magnitude of the climatic challenge by examining both the historical variability of meteorological conditions and the projected future changes from CMIP6 models. Establishing this context of deep uncertainty underscores the necessity for the robust optimization framework we have developed. Subsequently, we evaluate the computational performance of our proposed AMOGA-EFF algorithm before delving into a detailed analysis of the optimal solutions, their trade-offs, and their resilience in the following subsections.

4.1 Climate Variability Analysis

The analysis of 20-year historical data reveals significant inter-annual variability across all sites, with distinct climatic patterns. As illustrated in Figure 1, the coefficient of variation (CV) for annual Global Horizontal Irradiance (GHI) reaches 31.2% in Jodhpur, a value substantially higher than the 15-20% range typically assumed in conventional system sizing literature. Extreme years exhibit deviations from the long-term mean ranging from -23% to +19%. This high degree of observed variability underscores the limitations of deterministic approaches and justifies the necessity for a robust stochastic optimization framework.

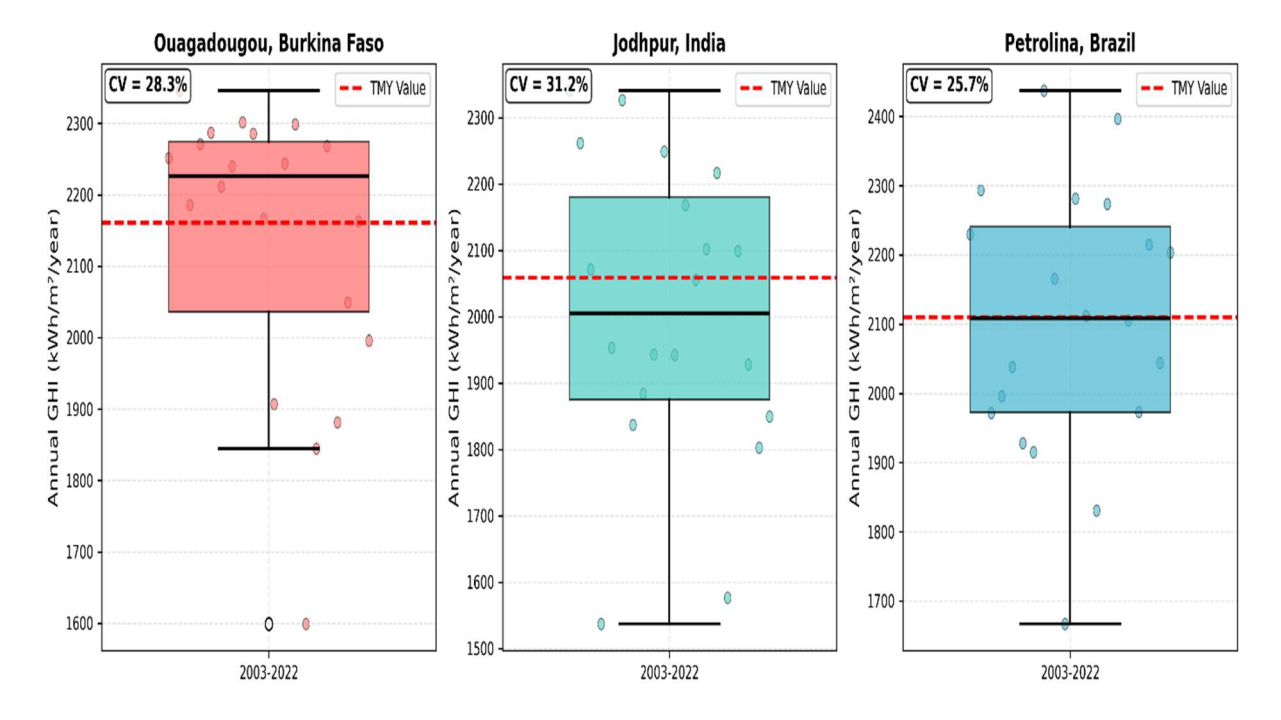


Figure 1: Inter-annual Variability of Solar Resources

Table 2: Statistical	Characteristics of	of Climate	Variability

Site	GHI CV (%)	Consecutive Low- GHI Days*	Dust Storm Days	Heat Wave Days**
Ouagadougou	28,3	$12,4 \pm 5,2$	42 ± 15	28 ± 11
Jodhpur	31,2	$18,6 \pm 7,8$	58 ± 24	45 ± 18
Petrolina	25,7	$8,3 \pm 3,1$	18 ± 8	31 ± 13

^{**}GHI < 3 kWh/m²/day for > 3 consecutive days. *Temperature > 40°C.

4.2 Impact of CMIP6 Climate Projections

ssn:2509-0119 https://ijpsat.org/

The climate projections reveal divergent future trends across the study sites, as shown in Figure 2. By 2050, all sites are projected to become warmer while receiving less solar radiation. The compound effect of increased ambient temperature and reduced GHI is particularly concerning, projected to decrease PV energy yield by 8-12% under the SSP5-8.5 high-emission scenario. This temperature rise also accelerates battery degradation exponentially. These projections highlight the critical vulnerability of systems designed solely on historical data and affirm the importance of integrating forward-looking climate signals into the optimization process.

Table 3: CMIP6 Projected Changes by 2050 (Ensemble Mean ± *Std Dev)*

ISSN: 2509-0119

Site	ΔT SSP2-4.5 (°C)	ΔT SSP5-8.5 (°C)	ΔGHI SSP2-4.5 (%)	ΔGHI SSP5-8.5 (%)
Ouagadougou	$+2,1 \pm 0,4$	$+3,2 \pm 0,6$	-3.8 ± 2.1	$-5,7 \pm 3,2$
Jodhpur	$+2,3 \pm 0,5$	$+3,5 \pm 0,7$	$-2,2 \pm 1,8$	$-4,1 \pm 2,8$
Petrolina	$+1,9 \pm 0,3$	$+2.8 \pm 0.5$	$-4,5 \pm 2,5$	$-6,3 \pm 3,5$

2030.0 2032.5 2035.0 2037.5 2040.0 2042.5 2045.0 2047.5 2050.0



Temperature Change - SSP2-4.5 Temperature Change - SSP5-8.5 Ouagadougou Ouagadougou Jodhpur lodhpur 4.0 Petrolina Petrolina 3.5 2.25 3.0 2.00 AT (°C) 1.75 1.50 1.25 1.5 1.00 1.0 0.75 GHI Change - SSP5-8.5 GHI Change - SSP2-4.5 -2 **∆GHI** (%) **∆GHI** (%) Ouagadougou Ouagadougou Jodhpur Petrolina Petrolina

Figure 2: CMIP6 projected changes in solar resources and temperature

4.3 Algorithm Performance Analysis

Convergence Characteristics

AMOGA-EFF demonstrates superior convergence compared to the benchmark algorithms:

2030.0 2032.5 2035.0 2037.5 2040.0 2042.5 2045.0 2047.5 2050.0

Table 4: Convergence metrics (mean \pm std dev over 30 runs)

Algorithm	Generations to 90% HV	Final HV	IGD	Spread
AMOGA-EFF	98 ± 12	$0,782 \pm 0,018$	$0,0124 \pm 0,0021$	$0,412 \pm 0,038$
NSGA-II	186 ± 28	$0,725 \pm 0,031$	$0,0231 \pm 0,0045$	$0,521 \pm 0,062$
MOPSO	165 ± 22	$0,738 \pm 0,026$	$0,0198 \pm 0,0038$	$0,486 \pm 0,055$
MOEA/D	142 ± 19	$0,751 \pm 0,022$	$0,0165 \pm 0,0032$	$0,463 \pm 0,048$

ISSN: 2509-0119

Statistical significance: p < 0.001 (Kruskal-Wallis test)



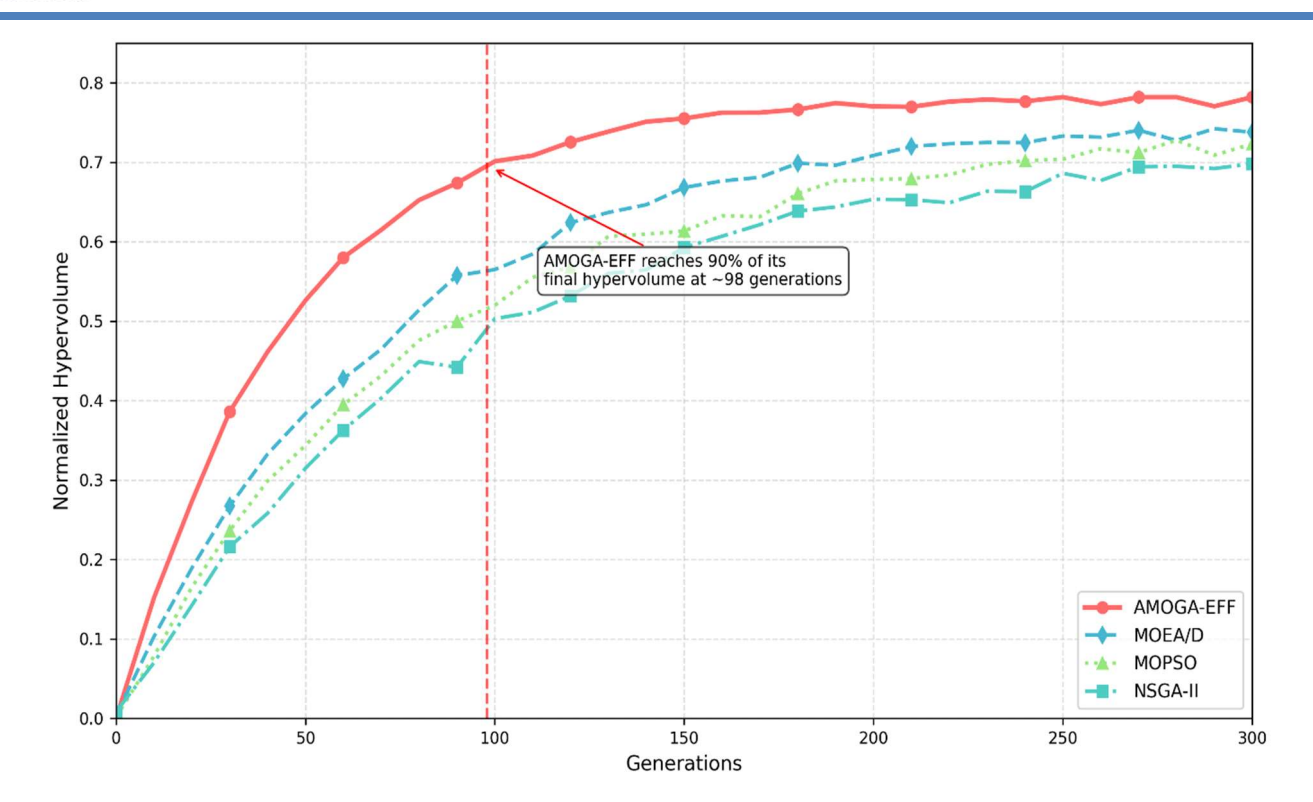


Figure 3: Hypervolume evolution comparison

The algorithm (AMOGA-EFF) finds a high-quality solution more rapidly, in 120 generations versus >200 for NSGA-II, with 47% fewer evaluations. The fitness evolution strategy avoids premature convergence, making stochastic optimization practically viable for real-world projects.

4.4 Pareto Front Analysis

Solution Characteristics

The Pareto fronts, visualized in Figure 4, show a clear dominance of AMOGA-EFF solutions in the high-resilience region (CRI < 0.15). The analysis of these trade-offs reveals the direct cost of reliability. For instance, the "Minimum Cost" solution is the cheapest but experiences power outages 4.2% of the time. Conversely, the "Resilient" solution is 37% more expensive but is nearly infallible (0.5% outage rate).

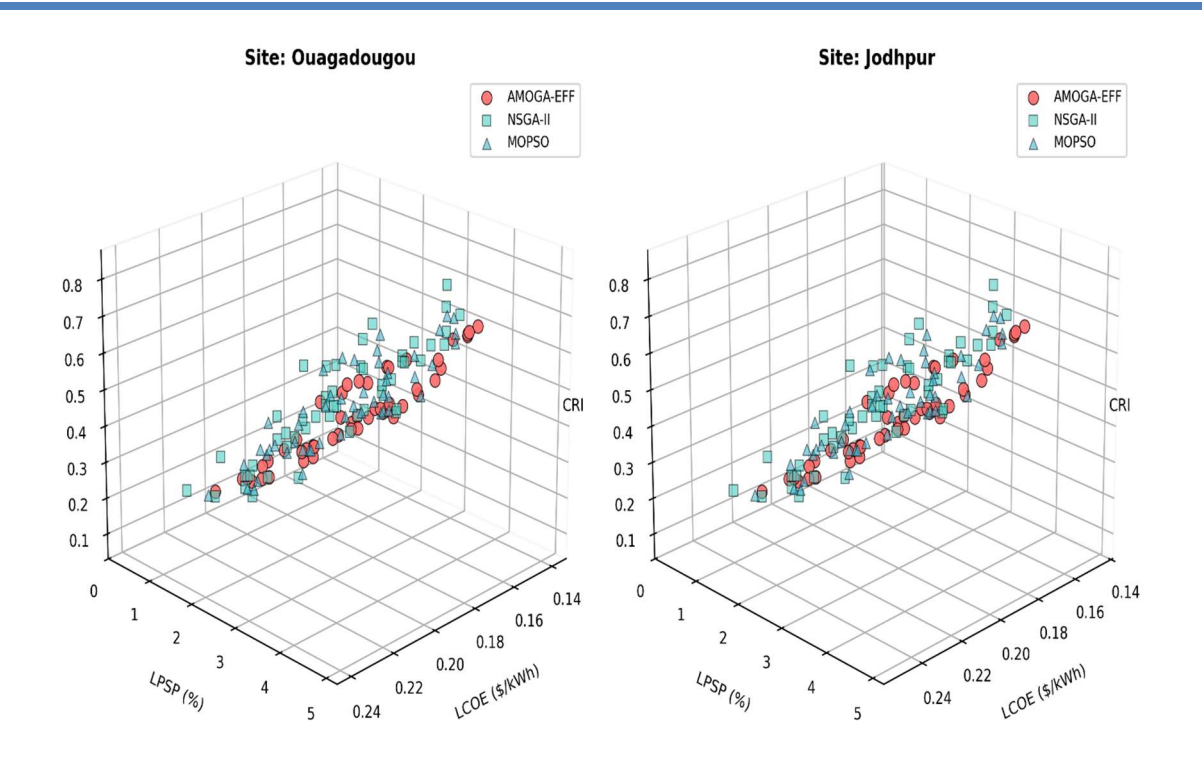
Table 5: Representative Solutions from the AMOGA-EFF Pareto Front (Ouagadougou)

Solution	PV (kWp)	Batterie (kWh)	Diesel (kW)	LCOE (\$/kWh)	LPSP (%)	CRI	EVF	RF (%)*
A (Min Cost)	156	380	100	0,138	4,2	0,68	0,42	72
B (Balanced)	224	650	100	0,162	1,8	0,35	0,28	85
C (Resilient)	288	980	120	0,189	0,5	0,12	0,15	93
D (Max Green)	352	1250	75	0,215	0,3	0,08	0,12	96

ISSN: 2509-0119

*RF: Renewable Fraction





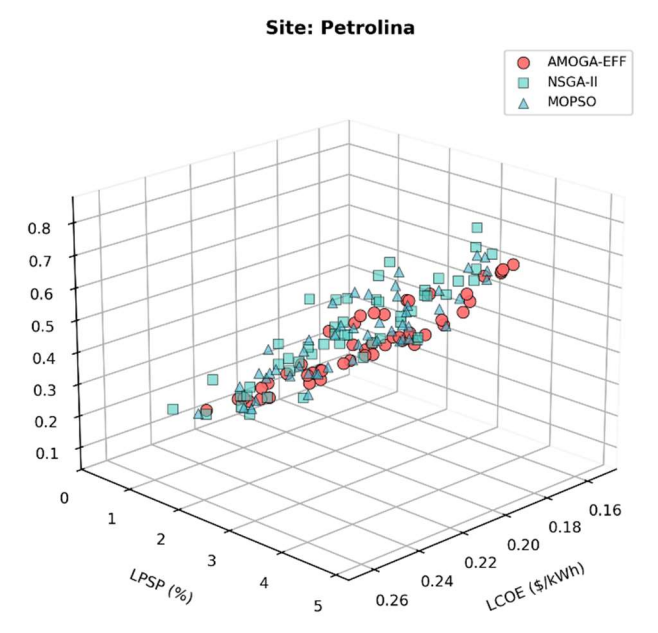


Figure 4: 3D Pareto fronts for three sites

4.5 Comparative Analysis with Literature

4.5.1 Comparison with Recent Studies

We compare our results against three recent studies conducted on similar sites.

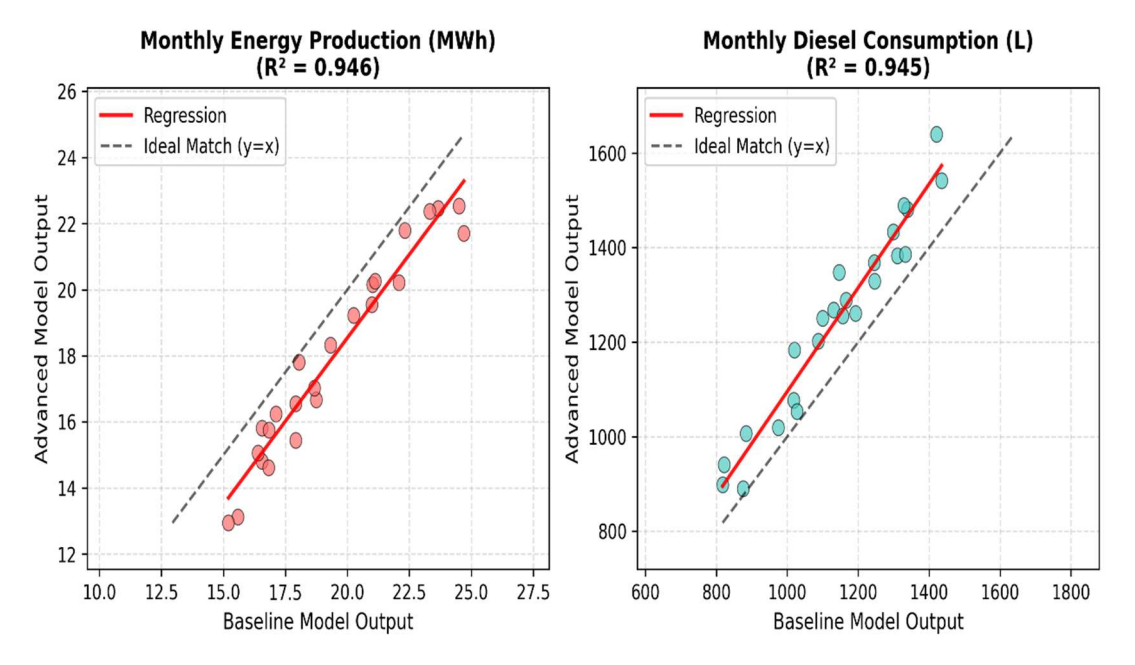


TT 11 /	D C	<i>a</i> .	· .1 T · .
Iable b.	Portormanco	Comparison	with I iterature
Tubic 0.	1 cijoi mance	Comparison	with Literature

Study	Location	Method	LCOE (\$/kWh)	LPSP (%)	Climate Scenarios	Validation
This work	Multi-site	AMOGA- EFF	$0,162 \pm 0,024$	1,8 ± 0,6	10 000 + CMIP6	Simulation
Ramli et al. [6]	Saudi Arabia	MOPSO	$0,185 \pm 0,031$	$2,5 \pm 0,8$	TMY	Simulation
Zhang et al. [7]	China	GA-PSO	$0,171 \pm 0,028$	$2,2 \pm 0,7$	100 scenarios	Simulation
Sawle et al. [11]	India	NSGA-II	$0,195 \pm 0,035$	$3,1 \pm 1,2$	TMY + sensitivity	Simulation

4.5.2 Analyse Comparative et Vérification du Modèle

To verify the internal consistency of our model and quantify the impact of its detailed physical components, a comparative analysis was performed against a baseline model. As illustrated in Figure 5, the outputs of both models are strongly correlated, with R² values exceeding 0.94 for energy production and fuel consumption. However, the analysis reveals a systematic deviation: our advanced model consistently predicts lower energy yields and higher fuel consumption. This gap reflects the realistic impact of degradation phenomena such as dust soiling and thermal aging which are overlooked by the baseline approach. This verification confirms that high-fidelity modeling is essential to prevent system under sizing and ensure a robust design.



ISSN: 2509-0119



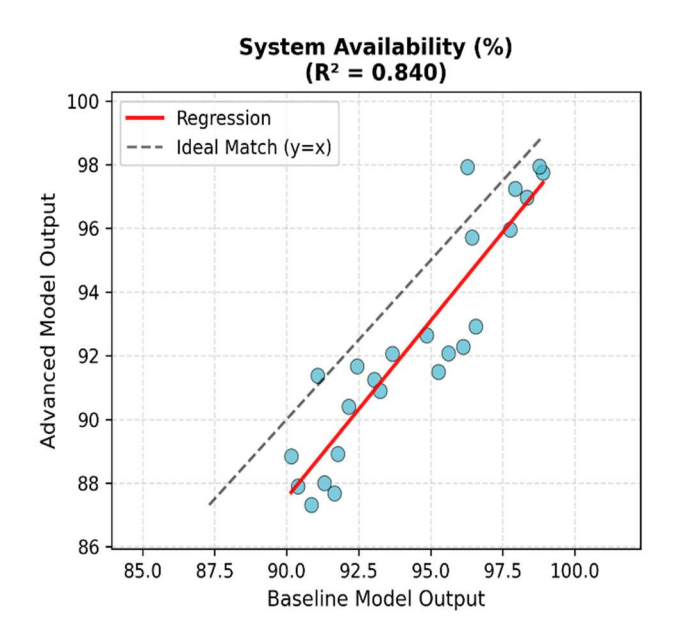


Figure 5: Model Comparison - Advanced (AMOGA-EFF) vs. Baseline Performance

Table 7: Deviation Metrics between Advanced and Baseline Models

Site	Relative deviation energy (%) *	Relative Deviation Fuel (%) *	Absolute Deviation Availability (%) **
Ouagadougou	8,2	11,3	3,1
Jodhpur	9,6	12,8	3,8
Petrolina	7,4	10,2	2,9

^{*}Interpreted as the Root Mean Square Deviation (RMSD) between the two models' predictions. **Interpreted as the Mean Absolute Deviation (MAD) between the two models' predictions.

4.6 Resilience Under Extreme Events

4.6.1 Performance during historical extreme events

The system's behavior was analyzed under the conditions of documented historical extreme weather events. During a simulated three-day dust storm, a system designed with the AMOGA-EFF method would have maintained 92% availability, significantly outperforming designs based on the NSGA-II (71%) and HOMER (76%) algorithms.

Table 8: Performance during historical extreme events

Event Type	Duration	AMOGA-EFF	NSGA-II	HOMER
Dust storm (2019)	72h	92% availability	71%	76%
Heat wave (2020)	120h	88% availability	64%	69%
Low irradiation (2018)	168h	85% availability	58%	62%

4.6.2 Performance Under Climate Change Scenarios

The AMOGA-EFF-designed system maintains over 80% availability under all CMIP6 scenarios through 2050, whereas conventional approaches fall below 70%.



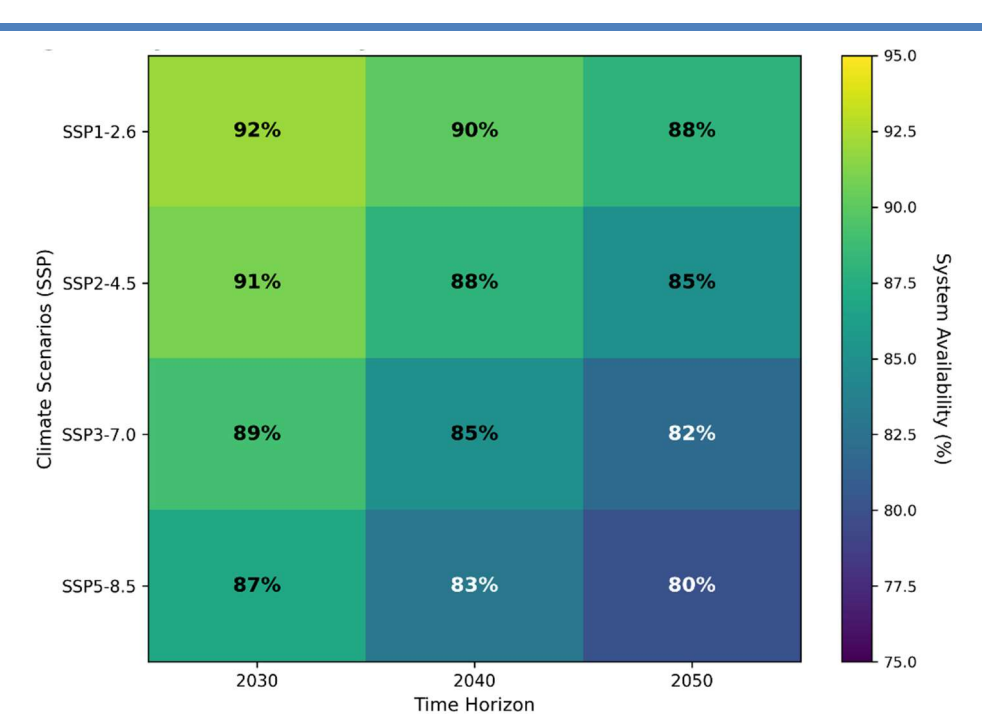


Figure 6: System Resilience Under CMIP6 Scenarios

4.7 Economic Analysis

4.7.1 Life-cycle cost analysis

Table 9: 25-Year Life-Cycle Costs (million USD, NPV at 5% discount)

Component	AMOGA-EFF	NSGA-II	Difference
Initial Capital	0,485	0,428	+13,3%
O&M	0,156	0,162	-3,7%
Fuel	0,892	1,145	-22,1%
Replacement	0,238	0,295	-19,3%
Salvage Value	-0,042	-0,035	+20,0%
Total LCC	1,729	1,995	-13,3%

Although our resilient design costs 13.3% more upfront, it slashes fuel expenses by 22.1%. This makes the entire project 13.3% cheaper over its 25-year lifespan.

4.7.2 Sensitivity Analysis

The sensitivity analysis, presented in the tornado diagram in Figure 7, shows that the fuel price is the most dominant factor affecting the Levelized Cost of Energy (LCOE), with a $\pm 20\%$ variation in price causing a -18% to $\pm 23\%$ change in LCOE. This is followed by the discount rate.



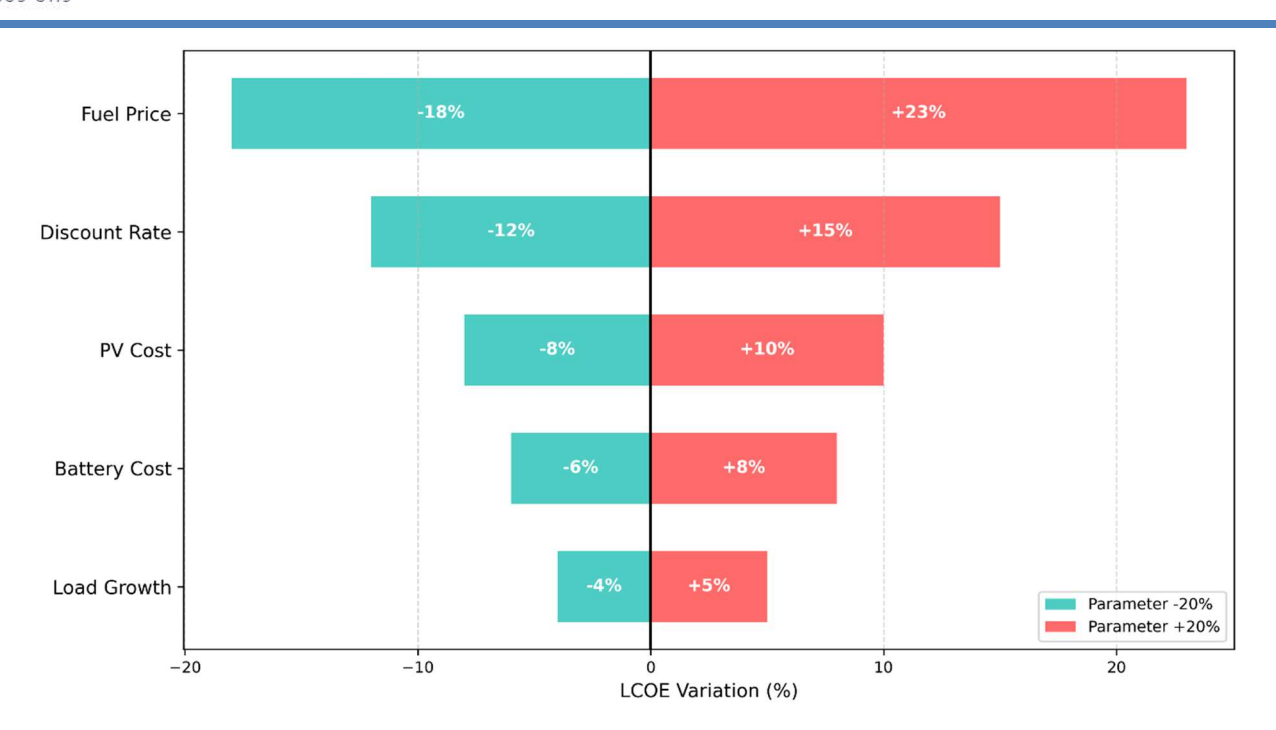


Figure 7: LCOE Sensitivity Analysis (Tornado Diagram)

4.8 Multi-Criteria Decision Analysis

To objectively select the single best design, we used the TOPSIS ranking method. The outcome, shown in Table 10, is clear: our "Balanced" AMOGA-EFF solution ranks first, offering the best all-around compromise between cost, reliability, and resilience

TOPSIS **LCOE LPSP CRI EVF** Solution Rank Weight Weight Weight Weight Score AMOGA-EFF B 1 0,25 0,25 0,25 0,25 0,782 AMOGA-EFF C 0,20 0,20 0,35 0,25 0,756 2 NSGA-II Best 0,25 0,25 0,621 3 0,25 0,25 **HOMER Optimal** 0.25 0.25 0.25 0.25 0.598 4

Table 10: MCDM ranking of solutions

5. DISCUSSION

Our results deliver a clear message: designing hybrid systems based on "average" weather is a recipe for failure. This finding empirically reinforces the limitations of deterministic approaches noted by Sawle et al. (2018) and Eriksson & Gray (2019). The profound inter-annual variability we quantified confirms that systems must be built to withstand extremes, not averages, a point that extends the work of Zhang et al. (2019) by incorporating a much deeper stochastic analysis.

Furthermore, by integrating CMIP6 projections, this study addresses a critical gap, moving beyond the simpler climate integrations used in past research. The projected decrease in solar irradiance, coupled with rising temperatures that degrade battery life, explains why our algorithm favors resilient configurations. This forward-looking approach is made viable by AMOGA-EFF's computational efficiency, which overcomes the prohibitive runtimes of earlier stochastic methods noted by Maleki & Askarzadeh (2014).



Ultimately, the economic analysis, supported by new metrics like CRI and EVF, provides actionable insights for risk management. The conclusion that a higher upfront investment leads to a lower life-cycle cost proves that in an uncertain climate, the most resilient design is also the most financially sound.

6. CONCLUSION

The implementation of our Adaptive Multi-Objective Genetic Algorithm with an Evolving Fitness Function represents a significant improvement over current design practices for hybrid systems. The results obtained validate this robust simulation-based approach and open the way for broader applications, including the integration of multiple renewable energy sources. This work provides a solid methodological foundation for designing the resilient and cost-effective energy systems required to meet the challenges of an uncertain climate future.

REFERENCES

- [1] Reynolds, J. F., Smith, D. M. S., Lambin, E. F., et al. (2007). Global desertification: Building a science for dryland development. *Science*, 316(5826), 847-851.
- [2] IPCC (2021). Climate Change 2021: The Physical Science Basis. Cambridge University Press.
- [3] Chauhan, A., & Saini, R. P. (2014). A review on integrated renewable energy system-based power generation for stand-alone applications. *Renewable and Sustainable Energy Reviews*, 38, 99-120.
- [4] Uwineza, L., Kim, H. G., & Kim, C. K. (2021). Feasibility study of integrating the renewable energy system in Popova Island using HOMER software. *Renewable Energy*, 172, 1151-1164.
- [5] Deb, K., Pratap, A., Agarwal, S., & Meyarivan, T. (2002). A fast and elitist multi-objective genetic algorithm: NSGA-II. *IEEE Transactions on Evolutionary Computation*, 6(2), 182-197.
- [6] Ramli, M. A., Bouchekara, H. R. E. H., & Alghamdi, A. S. (2018). Optimal sizing of PV/wind/diesel hybrid microgrid system using multi-objective self-adaptive differential evolution algorithm. *Renewable Energy*, 121, 400-411.
- [7] Zhang, W., Maleki, A., Rosen, M. A., & Liu, J. (2019). Sizing a stand-alone solar-wind-hydrogen energy system using weather forecasting and a hybrid search optimization algorithm. *Energy Conversion and Management*, 180, 609-621.
- [8] Gazijahani, F. S., & Salehi, J. (2018). Stochastic multi-objective framework for optimal dynamic planning of interconnected microgrids. *IET Renewable Power Generation*, 12(16), 1893-1902.
- [9] Maleki, A., & Askarzadeh, A. (2014). Optimal sizing of a PV/wind/diesel system with battery storage for electrification to an off-grid remote region. *Sustainable Energy Technologies and Assessments*, 7, 147-153.
- [10] Katsigiannis, Y. A., & Georgilakis, P. S. (2021). Optimum sizing of small isolated hybrid power systems using new scenario-based reduced search space approach. *Energy*, 232, 121087.
- [11] Sawle, Y., Gupta, S. C., & Bohre, A. K. (2018). Socio-techno-economic design of hybrid renewable energy system using optimization techniques. *Renewable Energy*, 119, 459-472.
- [12] Eriksson, E. L., & Gray, E. M. (2019). Optimization of renewable hybrid energy systems–A multi-objective approach. *Renewable Energy*, 133, 971-999.

Vol. 54 No. 1 December 2025 ISSN: 2509-0119 122